Cancer Cell
Article

A Conditional Mouse Model for Malignant Mesothelioma

Johan Jongsma,[1] Erwin van Montfort,[1] Marc Vooijs,[1,4] John Zevenhoven,[1] Paul Krimpenfort,[1] Martin van der Valk,[2] Marc van de Vijver,[3] and Anton Berns[1,*]
[1]Department of Molecular Genetics, The Cancer Genomics Centre, The Centre for Biomedical Genetics
[2]Department of Experimental Animal Pathology
[3]Division of Diagnostic Oncology
The Netherlands Cancer Institute, Plesmanlaan 121, 1066 CX Amsterdam, The Netherlands
[4]Present address: Molecular Research Lab, Department of Pathology, University Medical Center Utrecht, Heidelberglaan 100, 3584 CX Utrecht, The Netherlands.
*Correspondence: a.berns@nki.nl
DOI 10.1016/j.ccr.2008.01.030

SUMMARY

Malignant mesothelioma is a devastating disease that has been associated with loss of Neurofibromatosis type 2 (*NF2*) and genetic lesions affecting *RB* and *P53* pathways. We introduced similar lesions in the mesothelial lining of the thoracic cavity of mice. Mesothelioma developed at high incidence in *Nf2*;*Ink4a*/*Arf* and *Nf2*;*p53* conditional knockout mice with median survival times of approximately 30 and 20 weeks, respectively. Murine mesothelioma closely mimicked human malignant mesothelioma. Conditional *Nf2*;*Ink4a*/*Arf* mice showed increased pleural invasion compared to conditional *Nf2*;*p53* mice. Interestingly, upon *Ink4a* loss in the latter mice median survival was significantly reduced and all tumors were highly invasive, suggesting that *Ink4a* loss substantially contributes to the poor clinical outcome of malignant mesothelioma.

INTRODUCTION

Human malignant mesothelioma (MM) is an aggressive tumor strongly associated with asbestos exposure (Knudson, 1995; Liu et al., 2000; Murthy and Testa, 1999; Tiainen et al., 1989). In view of the long latency period between exposure and disease onset, the number of patients presenting with MM is expected to rise in the coming decade and peak around 2015 (Murthy and Testa, 1999; Hodgson et al., 2005). Pleural MM is the most prevalent form of human MM, while peritoneal and pericardial MM are less frequently seen. MM can be subdivided into three histological types, i.e., epithelial, sarcomatoid, and mixed. Sarcomatoid MM cannot always easily be discriminated from the various other sarcomas that can arise in the thoracic cavity, e.g., leiomyosarcomas, rhabdomyosarcomas, and osteosarcomas (Attanoos et al., 2000; Cagle et al., 1989). In addition, it can also be difficult to discriminate reactive fibroblast proliferations from sarcomatoid MM. In order to obtain a formal diagnosis of the different subtypes, histological specimens are required to assess both tumor morphology in combination with a set of (immunohistochemical) markers (Cagle et al., 1989; Carter and Otis, 1988; Khalidi et al., 2000; Ordonez and Tornos, 1997). Many markers have been tested to date but no single marker can classify with certainty a tumor as a MM (Ordonez, 1999). Although chemotherapy can lead to an improvement of overall and progression-free survival, this therapy is not curative and patients with MM usually succumb from the disease within a year after diagnosis (Knudson, 1995; Liu et al., 2000; Murthy and Testa, 1999; Tiainen et al., 1989).

There is an urgent need for experimental models of MM that can be used to not only study the onset and progression of the disease, but also to serve as a model to select new combination therapies and targeted agents. Different genetic lesions have been found associated with human MM (Ascoli et al., 2001; Lee and Testa, 1999; Sandberg and Bridge, 2001). Loss of the tumor suppressor genes (TSG) *INK4A* and *P14ARF*, Neurofibromatosis

SIGNIFICANCE

Malignant mesothelioma is a devastating disease related to asbestos exposure. Although some improvements in survival have been achieved, most patients die within 2 years after diagnosis. With the availability of new therapeutic agents with high specificity, there is a clear need for mouse models that closely reproduce the disease as observed in man. Here we describe the generation of such models. The models show a high incidence of mesothelioma with a relatively short latency. Tumor induction is initiated by locotemporal somatic inactivation of tumor suppressor genes found defective in human mesothelioma. Our mouse models should be suitable to further dissect the pathways critically important in mesothelioma development and progression and serve as invaluable tools to test new intervention strategies.

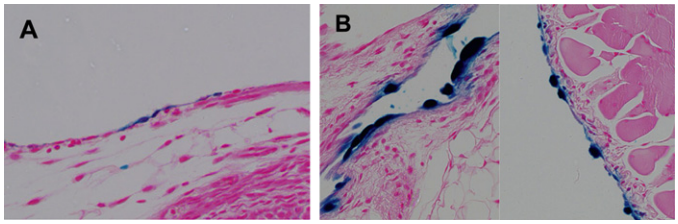

Figure 1. Mesothelium-Specific Targeting of Cre Activity after Intrathoric Administration of Adeno Viruses

(A) Mesothelium-specific recombination of the LacZ reporter transgene in R26R reporter mice injected in thoracic cavity with 1×10^9 pfu of Adeno-Cre virus indicated that mesothelial cells can be efficiently infected using this protocol. Occasional staining was observed in the muscle cell layer adjacent to the mesothelial cell lining. Virtually no staining was seen in the lung parenchyma.

(B) Intrathoracic injections of WT FVB mice with Adeno-LacZ virus showed a comparable β-galactosidase staining pattern, albeit stronger compared to the β-galactosidase expression levels induced by Cre recombinase in the R26R mice.

type 2 gene (*NF2*), *TRP53*, and possibly *RB* have been implicated (Bianchi et al., 1995; Carbone et al., 1997; Cheng et al., 1994; De Rienzo et al., 2001; Lechner et al., 1997; Mor et al., 1997; Papp et al., 2001; Prins et al., 1998; Sekido et al., 1995). Expression of SV40 T-antigen in pleural MM has been reported, suggesting that inactivation of pocket protein and *TP53* pathways may be important in the development of MM (De Luca et al., 1997). However, SV40 T-antigen is only sporadically reported to be expressed in MM and its contribution to the development of MM as an causative factor has been refuted (Hubner and Van Marck, 2002; Lopos-Rios et al., 2004). A number of groups have induced MM in mice, rats, and hamsters through aerosolic administration or injection of asbestos (Adamson et al., 1993; Craighead et al., 1987; Fleury-Feith et al., 2003; Libbus et al., 1988; Marsella et al., 1997; Sandhu et al., 2000) or through exposure to SV40 virus (Cicala et al., 1993; Rizzo et al., 2001). However, the MM induced in rats by aerosolic exposure to asbestos fibers did not show evidence for the loss of function of genes affected in human MM or known nuclear targets of SV40 Tag (Adamson et al., 1993; Craighead et al., 1987; Libbus et al., 1988; Marsella et al., 1997; Sandhu et al., 2000).

We decided to determine whether mutations affecting the same pathways found disrupted in human MM would also cause MM in mice. Therefore, we generated mutant mice carrying a range of single and compound lesions in the Nf2, p53, and Ink4a pathways with the expectation that such mice might serve as a suitable model for MM in man. In addition, this would allow us to study other (un)known genes that might play an important role in the initiation and progression of MM in both mouse and man. *Ink4a/Arf* and *Trp53* are TSG that are well known for their role in cell-cycle regulation (Sharpless and Chin, 2003). The *NF2* gene product, merlin or schwannomin (Nf2), belongs to the band 4.1 family of cytoskeletal-associated ERM proteins (Bianchi et al., 1994; Claudio et al., 1994a, 1994b, 1995; Gusella et al., 1999; Rouleau et al., 1993; Tikoo et al., 1994; Trofatter et al., 1993) and is thought to be involved in the organization of the actin cytoskeleton (Brault et al., 2001; Deguen et al., 1998; den Bakker et al., 2000; Sainio et al., 1997; Takeshima et al., 1994). It has been shown that reduced Nf2 expression lowers cell adhesion and induces Schwann cell proliferation, whereas enhanced expression of Nf2 leads to growth arrest (Gutmann et al., 1998, 1999). Nf2 is a phosphoprotein and its phosphorylation status can be modulated by numerous stimuli in culture, i.e., growth factor availability and cell-cell contact (Morrison et al., 2001; Shaw et al., 1998a, 1998b; Sherman and Gutmann, 2001). More recently, data on Nf2 function and its putative role in MM, i.e., Nf2's involvement in Ras/Rac signaling (Morrison et al., 2007) and signaling via PAK, which is a key modulator of cell motility (Kissil et al., 2002; Xiao et al., 2002), were published. Thus, Nf2 likely acts by linking cell adhesion to cell proliferation (Morrison et al., 2001). Loss of *Nf2* in mice has been shown to induce a variety of tumors with high metastatic potential (Giovannini et al., 1999, 2000; McClatchey et al., 1998). In addition, MM often show inactivation of the *INK4A;ARF* locus. Therefore, we focused on the inactivation of these loci. In view of the role of $p16^{INK4A}$ in the RB pathway and $p14^{ARF}$ in the TRP53 pathway, we included in the analysis compound mutants in which *Rb* and *Trp53* were also affected.

To circumvent the pleiotropic effects or embryonic lethality associated with *Ink4a/Arf* and *Trp53* or *Nf2* homozygous germline gene disruption in mice (Giovannini et al., 2000; McClatchey et al., 1997; Serrano et al., 1996), we employed conditional knockout (CKO) mice for *Nf2*, *Trp53*, *Rb*, and *Ink4a/Arf* TSG using the Cre-*Lox*P system (Akagi et al., 1997; Jonkers and Berns, 2002; Jonkers et al., 2001; Loonstra et al., 2001; Meuwissen et al., 2001). We sought to limit the inactivation of the conditional TSG through locotemporal introduction of adenoviruses encoding the site-specific recombinase Cre, i.e., Adeno-Cre (Akagi et al., 1997; Anton and Graham, 1995; Shibata et al., 1997). We and others have shown that replication defective adenoviruses will efficiently infect most cell types in vivo and elicit efficient gene recombination (Jackson et al., 2001; Meuwissen et al., 2001; Shibata et al., 1997).

Here, we describe the generation of a mouse model for sporadic MM utilizing direct injection of Adeno-Cre virus in the pleural cavity of adult mice carrying conditional TSG knockout alleles for *Nf2*, *p53*, *Rb*, and *Ink4a/Arf*.

RESULTS

Mesothelium-Specific Recombination in the Thoracic Cavity

Injection of Adeno-Cre into the thoracic cavity of Rosa26 LacZ (R26R) reporter mice (Soriano, 1999) resulted in β-galactosidase expression of the mesothelial linings (Figure 1A), indicating that mesothelial cells can be efficiently infected. Occasional staining was observed in the muscle cell layer underneath the mesothelial cell lining. Virtually no staining was seen in the lung parenchyma. Intrathoracic injections of wild-type (WT) FVB mice with Adeno-LacZ virus (Figure 1B) showed a comparable β-galactosidase staining pattern. A small amount of adenovirus might end up in the circulation and can give rise to tumors elsewhere (see below).

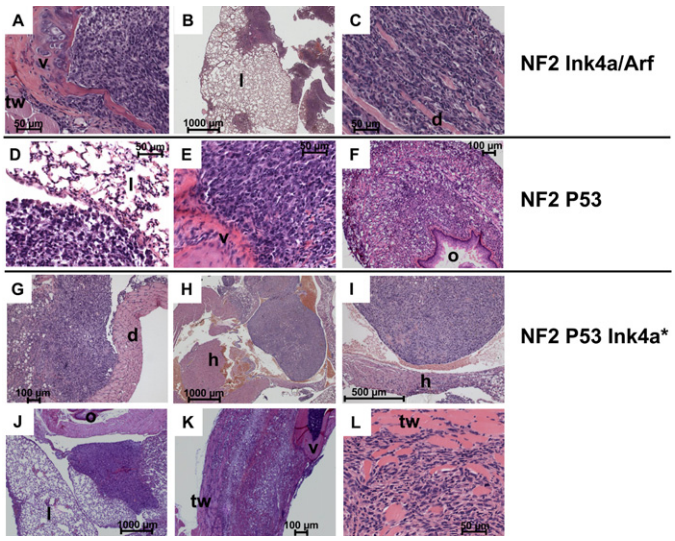

Figure 2. Overview of the MM Tumor Spectrum Induced by Adeno-Cre Virus in the Different Genetic Backgrounds

The epitheloid, sarcomatoid, and mixed tumors were found with variable frequency, depending on the different genetic backgrounds. The invasive tumors in the $Nf2^{F}$;*Ink4a/Arf*^{F} mice were almost all of the sarcomatoid type, although nodular tumors were also observed near the invasive tumors (A, B, and C). Examples are shown for vertebrae invasion (A), lung invasion (B), and invasion of the diaphragm (C). In the $Nf2^{F}$;$p53^{F}$ mice, tumors ranged from nodular, noninvasive visceral to nodular, locally invasive visceral and invasive parietal growth patterns. In the sarcomatoid tumors invading muscle layers, a typical "signet-cell"-like picture was observed, especially when cells invaded the esophagous. Some tumors grew as large nodular tumors on the chest wall, whereas others grew at multiple sites along the lung mesothelial cell layer (D, E, and F). Examples are shown for a nodular, noninvasive tumor (D), a vertebrae-invading tumor (E), and a local invasive tumor invading the muscularis and submucosa of the esophagous (F). The addition of the conventional *Ink4a** knockout to $Nf2^{F}$;$p53^{F}$ mice created the spectrum of nodular, invasive, and aggressive tumor growth at both the lung mesothelial cell layer as well as in the chest wall and diaphragm (G, H, I, J, K, and L). Examples are shown for a tumor growing along the diaphragm (G), a tumor growing inside the atrium of the heart (H and I), tumors invading either the lungs or the thoracic wall (J and K), and thoracic wall invasion (L). tw, thoracic wall; d, diaphragm; o, esophagus; l, lung; h, heart; v, vertebra. Bars for different magnifications are shown as burn in marks (Axiocam, Color-CCD camera).

Locotemporal Inactivation of Nf2 Together with Either Ink4a/Arf or p53 Gives Rise to a Variety of Tumors

We induced mesothelial-specific loss of *Nf2*, *Ink4a/Arf*, and *p53* TSG by locotemporal expression of Cre recombinase upon intrathoracic Adeno-Cre injection in mice. We used homozygous CKO for *Nf2*, *Ink4a/Arf*, and *p53*, and homozygous compound CKO *Nf2*;*Ink4a/Arf* and *Nf2*;*p53* carrying either an active or inactive *Ink4a* allele (*Ink4a**) (Krimpenfort et al., 2001) and matched heterozygous CKO mice. The tumors that arose in our mouse cohorts mainly comprised thoracic tumors (including MM, rhabdomyosarcomas, and schwannomas), lymphomas, or leukemia and leiomyomas of the uterus wall. Hepatomegaly was also frequently observed (see Table 1). A portion of the mice died of age-related or nonspecific causes, e.g., papillary lung tumor development or heart failure.

In $Nf2^{F/F}$;*Ink4a/Arf*$^{F/F}$ (n = 57), $Nf2^{F/F}$;$p53^{F/F}$ (n = 55), and $Nf2^{F/F}$;$p53^{F/F}$;*Ink4a*$^{*/*}$ (n = 51) mice, thoracic tumors were identified by H&E staining in 80%–100% of the mice (Figure 2). $Nf2^{F/F}$;$p53^{F/F}$ mice developed either nonaggressive epitheloid or mixed tumors with confined invasion of the visceral pleura or (sarcomatoid) tumors with strong invasion of both visceral and parietal pleura accompanied by pleural effusions, whereas $Nf2^{F/F}$;$p53^{F/F}$;*Ink4a*$^{*/*}$ as well as $Nf2^{F/F}$;*Ink4a/Arf*$^{F/F}$ mice almost exclusively developed highly invasive tumors.

We observed similar tumors in the heterozygous groups, i.e., $Nf2^{F/WT}$;*Ink4a/Arf*$^{F/F}$ (n = 41) mice, $Nf2^{F/F}$;*Ink4a/Arf*$^{F/WT}$ (n = 52) mice, $Nf2^{F/WT}$;$p53^{F/F}$ (n = 34) mice, and $Nf2^{F/F}$;$p53^{F/WT}$ (n = 20) mice as found in the homozygous group, except that the latency period was longer (Table 1). In $Nf2^{F/F}$;$p53^{F/F}$;*Ink4a*$^{*/WT}$ mice (n = 16), we observed aggressive thoracic tumor growth. The parietal pleura, i.e., chest wall and diaphragm often showed invasion with concomitant pleural effusions.

In 30 $Nf2^{F/F}$ mice and 13 $p53^{F/F}$;*Ink4a*$^{*/*}$ mice, we observed 5 and 2 MM-like thoracic tumors, respectively, whereas these were not observed in 19 $p53^{F/F}$ mice and 17 *Ink4a/Arf*$^{F/F}$ mice.

Hepatomegaly either due to oval cell hyperplasia, cholangiocarcinomas and/or hepatomas, and leiomyomas of the uterus were observed throughout all genotypes carrying $Nf2^{F/F}$ alleles except in $Nf2^{F/F}$;$p53^{F/F}$;*Ink4a*$^{*/*}$ and $Nf2^{F/F}$;$p53^{F/F}$;*Ink4a*$^{*/WT}$ mice that succumbed to MM before the onset of hepatomegaly or leiomyoma (Table 1). A few thymic lymphomas were observed in $Nf2^{F/F}$;$p53^{F/F}$ and $Nf2^{F/F}$;$p53^{F/WT}$, whereas monocytic myeloid leukemias (MML) were found in four $Nf2^{F/F}$;*Ink4a/Arf*$^{F/F}$, eight $Nf2^{F/F}$;*Ink4a/Arf*$^{F/WT}$ and 22 $Nf2^{F/WT}$;*Ink4a/Arf*$^{F/F}$ mice (see Table 1). $p53^{F/F}$ mice primarily developed malignant lymphomas, osteosarcomas, or leiomyosarcomas, whereas *Ink4a/Arf*$^{F/F}$ mice developed mostly MML as well as leiomyosarcomas. The *Ink4a*$^{*/*}$;$p53^{F/F}$ mice primarily developed malignant lymphomas from spleen with spreading to liver and lungs. The occurrence of other tumors is due to infection of other cell types that are known to be particularly susceptible to tumor development upon deletion of these TSG. Spreading of a small amount of Adeno-Cre then suffices to induce these tumors, especially in genotypes in which MM development is delayed.

Immunohistochemistry of Epitheloid, Sarcomatoid, and Mixed Murine MM in the Different Compound Mutants

Immunohistochemistry (IHC) of the thoracic tumors in *Nf2*;*Ink4a/Arf*, *Nf2*;*p53*, and *Nf2;p53*;*Ink4a** cohorts allowed us to discriminate between MM, rhabdomyosarcomas, and schwannomas. MM stained positive for pankeratin, keratin8, vimentin, and mesothelin and negative for Myf-4 (Figure 3). Some invasive tumors showed partly positive staining for smooth muscle actin due to local angiogenesis and S-100 due to invasion of tumor cells into peripheral nerve sheets (data not shown). In a few cases, a MM and a rhabdomyosarcoma were found in the same animal as reflected by keratin8 and Myf4 staining pattern (Figure 3). Alcian blue staining was performed with and without hyaluronidase treatment to identify MM in those cases where keratin 8, vimentin, and mesothelin stainings were inconclusive.

Table 1. Locotemporal Inactivation of *Nf2* Together with *Ink4a/Arf*, *p53*, or Both *p53* and *Ink4a* Gives Rise to a Variety of Tumors

	$Nf2^F;p53^F$			$Nf2^F;Ink4a/Arf^F$			$Nf2^F;p53^F;Ink4a^*$	
Genotype	het;hom (n = 34)	hom;hom (n = 55)	hom;het (n = 20)	het;hom (n = 41)	hom;hom (n = 57)	hom;het (n = 52)	hom;hom;het (n = 16)	hom;hom;hom (n = 51)
Tumor (site)								
Mice with thoracic tumors	21 (61.8)	47 (85.5)	8 (40.0)	14 (34.1)	47 (82.5)	18 (34.6)	15 (93.8%)	51 (100%)
MM, epithelial	5	7	3	4	1	4	0	0
MM, sarcomatoid	5	21	2	3	31	5	6	36
MM, mixed	10	17	0	7	13	9	9	11
Rhabdomyosarcoma	0	2	0	0	3	0	1	4
Schwannoma	1	1	3	0	1	0	0	1
Lymphoma, MML leukemia	3 (8.8)	4 (7.3)	5 (25.0)	22 (53.7)	4 (7.0)	8 (15.4)	0	0
Uterus wall tumor (leiomyoma)	3 (8.8)	4 (7.3)	5 (25.0)	7 (17.1)	2 (3.5)	8 (15.4)	0	0
Hepatomegaly	0	2 (3.6)	1 (4.0)	0	24 (42.1)	12 (23.1)	0	0
Aspecific tumor	7 (20.6)	6 (10.9)	2 (8.0)	10 (24.4)	2 (3.5)	10 (19.2)	1 (6.2)	0

Locotemporal inactivation of *Nf2* together with either *Ink4a/Arf*, *p53*, or both *p53* and *Ink4a* gives rise to a variety of tumors. Some mice were diagnosed with both MM and another tumor, e.g., rhabdomyosarcoma or schwannoma. The tumors in $Nf2^F;Ink4a/Arf^F$ and $Nf2^F;p53^F$ are arranged by genotype in three different columns, het;hom, hom;hom, and hom;het, respectively. For $Nf2^F;p53^F;Ink4a^*$, we only show the hom;hom;het and hom;hom;hom combinations. Aspecific tumors are tumors that have not been induced by adenoCre virus, e.g., papillary lung tumors. Hom, homozygous; het, heterozygous.

Subdivision of the MM into (1) epitheloid nodular tumors invading local visceral pleura, (2) sarcomatoid tumors invading both the visceral and parietal pleura, and (3) mixed epitheloid and sarcomatoid tumors invading either the visceral or parietal pleura was performed for all cohorts. Epithelial MM was found in $Nf2^{F/F}$;$p53^{F/F}$ and $Nf2^{F/F}$;$Ink4a/Arf^{F/F}$ mice, but not in $Nf2^{F/F}$;$p53^{F/F}$;$Ink4a^{*/*}$ mice. Sarcomatoid MM and mixed MM were found in $Nf2^{F/F}$;$p53^{F/F}$, $Nf2^{F/F}$;$Ink4a/Arf^{F/F}$, and $Nf2^{F/F}$;$p53^{F/F}$;$Ink4a^{*/*}$ mice (Table 1).

Latency of MM Development

MM primarily arose in *Nf2*;*p53* or *Nf2*;*Ink4a/Arf* CKO mice. The Kaplan Meier survival curves of MM in *Nf2*;*Ink4a/Arf*, *Nf2*;*p53*, and *Nf2*;*p53*;*Ink4a** CKO mice are shown in Figure 4. MM in *Nf2*;*Ink4a/Arf* CKO mice showed a shorter latency period in comparison to both heterozygous groups (Figure 4A). Median survival time ranged from 220 days in *Nf2*;*Ink4a/Arf* CKO mice to 410 and 495 days in mice carrying one WT *Nf2* or *Ink4a/Arf* allele, respectively. MM development in homozygous *Nf2*;*p53* conditional mutants was accelerated compared to matched heterozygotes (Figure 4B). Median survival time ranged from 135 days in *Nf2*;*p53* homozygous mice to 215 and 605 days in mice carrying one WT *Nf2* or *p53* allele, respectively.

These observations indicate that loss of *Nf2*, *p53*, or *Ink4a/Arf* each substantially contribute to development of MM. By comparing the full CKO mice in Figures 4A and 4B, a clear shift is seen in tumor latency, i.e., median survival time of 220 days (*Nf2*;*Ink4a/Arf*) compared to 135 days (*Nf2*;*p53*).

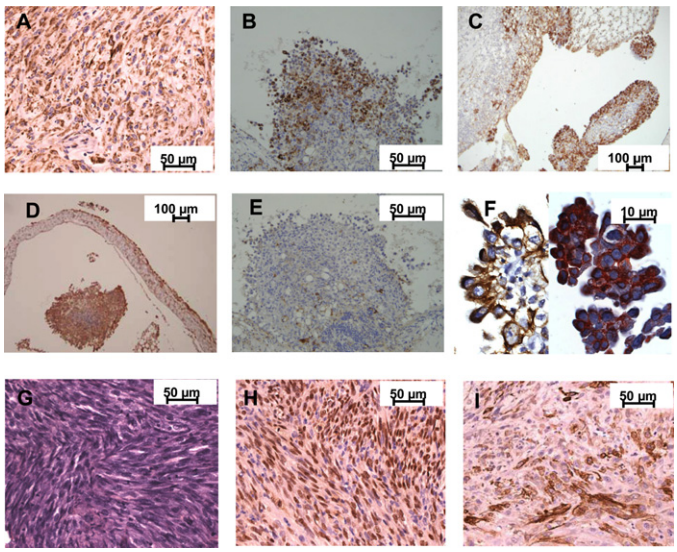

Figure 3. IHC Analysis of Murine Thoracic Sarcomatoid Tumors
The sarcomatoid tumors that stained positive for pankeratin (A), keratin 8 (B and C), and mesothelin (D) and negative for Myf-4 (E) were designated as MM. The commonly used combined expression of keratin (left, DAB [diaminobenzidine]) and vimentin (right, AEC [3-amino-9-ethylcarbazole]) by mesothelial cells is also shown (F). Other tumor types are a few rhabdomyosarcomas ([G], HE-staining; [H], Myf4-positive) or leiomysarcoma ([I], SMA-positive). Bars for different magnifications are shown as burn in marks (Axiocam, Color-CCD camera).

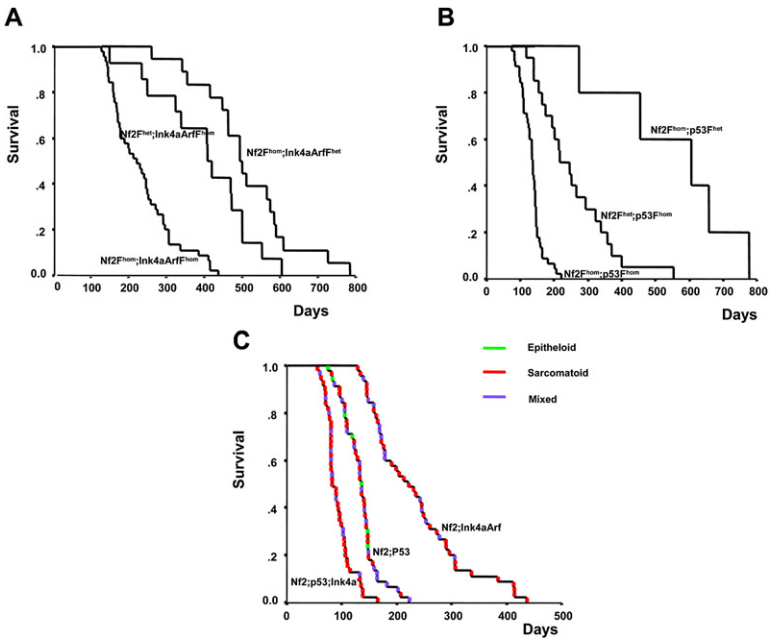

Figure 4. The Latency Curves for Tumors Arising after Intrathoracic Adeno-Cre Injections in Conditional *Nf2*;*Ink4a/Arf*, *Nf2*;*p53*, and *Nf2*;*p53*;*Ink4a Mice**

(A) Kaplan Meier analysis for survival in days by genotype is shown in the upper left panel for the *Nf2*;*Ink4a/Arf* combinations. MM latency in *Nf2*;*Ink4a/Arf* homozygous CKO mice clearly shifted to the left in comparison with either heterozygous control group. For the *Nf2*;*Ink4a/Arf* mice, median survival time ranged from 220 days in *Nf2*;*Ink4a/Arf* homozygous CKO mice compared to 410 and 495 days in mice carrying one WT *Nf2* or *Ink4a/Arf* allele, respectively. *Nf2*;*Ink4a/Arf* homozygous CKO significantly differed from both control groups (log rank test, $p < 0.00001$) as well as both heterozygous groups differed from each other (log rank test, $p < 0.035$).

(B) Kaplan Meier analysis for survival in days by genotype are shown in the upper right panel for the *Nf2*;*p53* combinations. MM latency in *Nf2*;*p53* homozygous CKO mice also clearly shifted to the left in comparison to both heterozygous control groups. For the *Nf2*;*p53* mice, median survival time was 135 days in *Nf2*;*p53* homozygous CKO mice compared to 215 and 605 days in mice carrying one WT *Nf2* or *p53* allele, respectively. *Nf2*;*p53* homozygous CKO mice significantly differed from both control groups (log rank test, $p < 0.00001$) as well as both heterozygous groups differed from each other (log rank test, $p < 0.0025$).

(C) Inclusion of the *Ink4a** knockout allele (Krimpenfort et al., 2001) in *Nf2*;*p53* CKO mice shifted the tumor latency curve for these mice strikingly to the left. Red, purple, and green colors mark sarcomatoid tumors growing invasive in both parietal and visceral pleura, mixed tumors locally invasive in visceral pleura, and nodular tumors locally invasive in visceral pleura, respectively. Note that most tumors in the left curve are invading both parietal and visceral pleura.

In Figure 4C, median survival time was 80 days in $Nf2^{F/F}$;$p53^{F/F}$;$Ink4a^{*/*}$ mice compared to 135 and 220 days in *Nf2*;*p53* and *Nf2*;*Ink4a/Arf* CKO mice, respectively. All three groups differed significantly (log rank test, $p < 0.00001$).

Interestingly, we observed a marked difference in the aggressiveness of the tumors between genotypes. Whereas the most aggressive phenotype was observed in *Nf2*;*Ink4a/Arf* tumors (70%), a substantial variation in malignancy, i.e., in invasive behavior, was seen in *Nf2*;*p53* tumors. This led to the question whether loss of function of *Ink4a* might be responsible for the increased malignancy of *Nf2*;*Ink4a/Arf* tumors.

To answer this question, the *Ink4a** allele, which is functional for *Arf*, was crossed into $Nf2^{F/F}$;$p53^{F/F}$ mice. In $Nf2^{F/F}$;$p53^{F/F}$;$Ink4a^{*/*}$ mice, the tumor latency was markedly reduced as compared to $Nf2^{F/F}$;$p53^{F/F}$ mice (Figure 4C). Median survival time was 80 days in $Nf2^{F/F}$;$p53^{F/F}$;$Ink4a^{*/*}$ mice compared to 135 and 220 days in $Nf2^{F/F}$;$p53^{F/F}$ and $Nf2^{F/F}$;$Ink4a/Arf^{F/F}$ mice, respectively. Note that most of the tumors induced in $Nf2^{F/F}$;$p53^{F/F}$;$Ink4a^{*/*}$ mice (75%) are highly malignant as observed by both parietal and (local) visceral pleural invasion, whereas only half of the tumors induced in $Nf2^{F/F}$;$p53^{F/F}$ mice shows invasion of both visceral and parietal pleura and one-third shows local invasion of the visceral pleura only. *Ink4a* loss, thus, seems to confer a more aggressive behavior to murine MM cells. This is accompanied by pleural effusions, invasive tumor growth into the parietal pleura of the chest wall, the esophagus or intestine causing gastro-intestinal obstruction, and subsequent weight loss leading to a shorter latency period.

IHC for $p16^{Ink4a}$ Expression in Murine MM

In order to investigate whether $p16^{Ink4a}$ expression in murine MM is directly correlated with tumor malignancy, we performed IHC for $p16^{Ink4a}$ in tumors induced in $Nf2^{F/F}$;$p53^{F/F}$ mice with and without invasive/aggressive growth features. Most of the nodular and local visceral pleura invading tumors showed strong nuclear staining for $p16^{Ink4a}$ (Figure 5A). Some of the invasive counterparts in the parietal pleura of these tumors showed either a patchy staining pattern focused at the edges of tumor invasion or a strong reduction in nuclear staining (Figure 5B). Other invasive parietal pleural tumors stained completely negative for $p16^{Ink4a}$, and a few showed strong nuclear staining in the more invasive parietal part of the tumor. As expected, tumors induced in $Nf2^{F/F}$;$Ink4a/Arf^{F/F}$ mice did not stain for $p16^{Ink4a}$, validating the specificity of our antibody (Figure 5C). In $Ink4a^{*/WT}$ tumors, we did observe strong nuclear staining in the nodular tumors (Figure 5D), presumably caused by the remaining WT *Ink4a* allele, whereas in some of the invasive counterparts in the parietal pleura, the $p16^{Ink4a}$ protein staining was reduced. In $Ink4a^{*/*}$ homozygous tumors, no $p16^{Ink4a}$ expression was observed (Figure 5E).

We also analyzed the methylation status of the *Ink4a* allele in MM induced in $Nf2^{F/F}$;$p53^{F/F}$ and $Nf2^{F/F}$;$p53^{F/F}$;$Ink4a^{*/WT}$ tumors to verify whether a correlation could be found between methylation and malignancy of the *Nf2*;*p53* tumors. To exclude contamination with normal cells, we used primary cell cultures of mesothelial tumors and could show *Ink4a* promotor methylation in only 1 out of 9 tumors in $Nf2^{F/F}$;$p53^{F/F}$ mice (data not shown), indicating that epigenetic inactivation of *Ink4a* is unlikely to contribute significantly to MM development in tumors of $Nf2^{F/F}$;$p53^{F/F}$ mice, although loss of *Ink4a* accelerates tumor onset and augments malignancy. In none of the $Nf2^{F/F}$;$p53^{F/F}$;$Ink4a^{*/WT}$ tumors (14 tested) were we able to show methylation of the $Ink4a^{WT}$ allele, which is in agreement with findings of Sharpless et al. who could also not detect methylation of the WT allele in heterozygous *Ink4a* mutants (Sharpless et al., 2002).

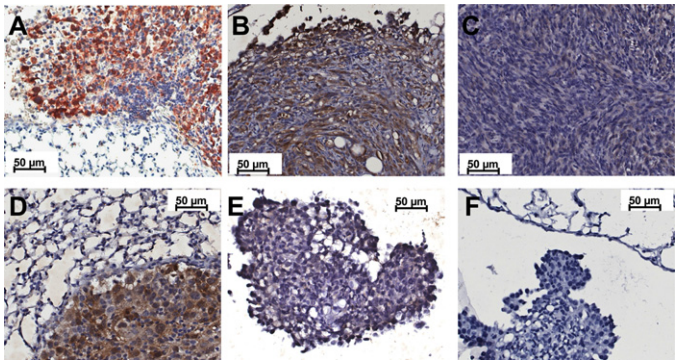

Figure 5. IHC Analysis of p16^{Ink4a} Expression in Murine MM

(A) IHC for p16^{Ink4a} in *Nf2*;*p53* tumors with and without invasive/aggressive growth features. Most of the nodular and local visceral pleura invading tumors showed strong nuclear staining for p16^{Ink4a}.

(B) Some of the invasive counterparts in the parietal pleura of these *NF2*;*p53* tumors showed either a patchy staining pattern of the tumors or a strong reduction of nuclear staining with slightly increased staining at the edges of the tumors.

(C) Other invasive parietal pleural tumors stained completely negative for p16^{Ink4a} and a few showed strong nuclear staining in the more invasive parietal part of the tumor. *Nf2*;*Ink4a*/*Arf* tumor cells stained completely negative for p16^{Ink4a}.

(D) In *Ink4a** heterozygous tumors we did observe strong nuclear staining of WT p16^{Ink4a} in the nodular tumors.

(E and F) In *Ink4a** homozygous tumors we observed no staining of the mutant protein (E) when compared to PBS control (F). Bars for different magnifications are shown as burn in marks (Axiocam, Color-CCD camera).

Assessment of Biallellic Recombination or Loss of Heterozygosity of Nf2, p53, or Ink4a in Murine MM Development

MM arising in mice carrying combinations of conditional *Nf2*, *Ink4a*/*Arf*, and *p53* alleles were analyzed for Cre-mediated recombination and loss of heterozygosity (LOH) by Southern blotting. *Nf2*, *p53*, and *Ink4a*/*Arf* status were determined in tissue samples from all above mentioned groups. Most tumor samples in the *Nf2*;*p53* and *Nf2*;*p53*;*Ink4a** cohorts showed Adeno-Cre-induced partial deletion of the *Nf2* exon 2 (Figure 6A). We ascribe this apparent partial recombination to contamination with surrounding WT cells (see below). This contamination was highest in the more invasive tumors. A similar observation was made for Cre-induced recombination of *p53* in both cohorts (Figure 6B). Tissue culture-propagated cells derived from either pleural effusions or primary tumors showed complete recombination of conditional *Nf2* or *p53* alleles and LOH of the WT *Nf2* allele in the case of heterozygotes. Likewise, the tumors in the *Nf2*$^{F/F}$;*Ink4a*/*Arf*$^{F/F}$ cohort exhibited partial *Ink4a*/*Arf* and *Nf2* recombination. The levels of recombination of both alleles was comparable (data not shown). Tissue culture propagated and soft-agar cloned cells derived from either pleural effusions or primary tumor showed complete recombination of both conditional alleles and LOH of the WT *Nf2* allele in case of a *Nf2*$^{F/WT}$ germline configuration. The sometimes limited recombination of *Nf2* and *Ink4a*/*Arf* in primary tumors is likely caused by stromal contamination in view of the similar extent of recombination of the different TSG and the subsequently complete recombination observed after in vitro propagation of the tumors (data not shown). In a few *Ink4a*$^{*/WT}$ samples, we were not able to detect the remaining WT *Ink4a* allele in *Nf2*$^{F/F}$;*p53*$^{F/F}$;*Ink4a*$^{*/WT}$ tumors (data not shown), which may indicate loss of the WT allele.

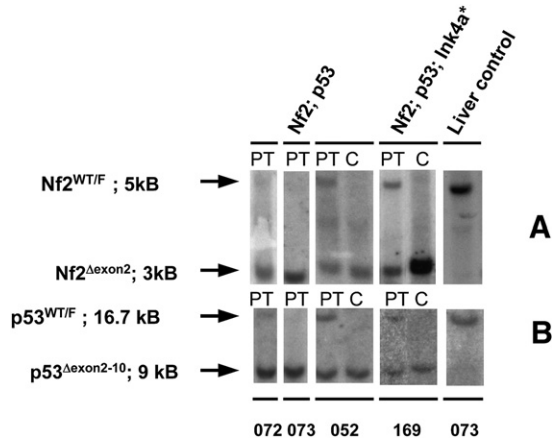

Figure 6. Biallelic Recombination and LOH Analysis for *Nf2*, *p53*, and *Ink4a* in Murine MM Samples

Nf2 and *p53* status were determined in tumor samples from *Nf2*;*p53*, *Nf2*;*p53*;*Ink4a**, and *Nf2*;*Ink4a*/*Arf* mice (A and B). Most tumor samples (PT) derived from *Nf2*;*p53*, and *Nf2*;*p53*;*Ink4a** CKO mice showed Adeno-Cre induced (partial) deletion of the *Nf2* exon 2 (A) as opposed to liver controls (L). Presence of the unrecombined allele in the analysis is likely due to contamination with DNA extracted from stromal cells. This contamination was highest in the more invasive tumors. The picture for Adeno-Cre-induced recombination of *p53* exons 2–10 is comparable in both cohorts (B). Tissue-culture-propagated cells (C) derived from either pleural effusions or primary tumor showed complete recombination of conditional *Nf2* or *p53* alleles and LOH of the WT *Nf2* and *p53* allele in the case of heterozygotes.

In Vivo Bioluminescent Imaging of Spontaneous Murine MM Development

After crossing in a luciferase reporter (LucR) (Lyons et al., 2003), we were able to follow the development of MM in both *Nf2*$^{F/F}$;*p53*$^{F/F}$ and *Nf2*$^{F/F}$;*p53*$^{F/F}$;*Ink4a*$^{*/*}$ mice noninvasively. An example of a bioluminescent primary tumor is shown in Figure 7A at 9 weeks after IT injection of Adeno-Cre virus. Through soft-agar cloning of primary tumor cell suspensions, we were able to generate clonal cell lines from all three genetic backgrounds with or without this LucR (see Supplemental Data available online, Table S1). The LucR^{+} clonal cell line derived from the primary tumor shown in Figure 7A gave rise to LucR^{+} tumors upon orthotopic grafting into syngeneic hosts (Figure 7B). Histological examination of H&E-stained sections of both primary (Figure 7C) and orthotopic tumor (Figure 7D) showed very similar growth and invasive characteristics.

DISCUSSION

We describe here the development of a conditional mouse model for human MM. To this end, we induced mesothelial-specific loss of *Nf2*, *Ink4a*/*Arf*, and *p53* TSG by locotemporal

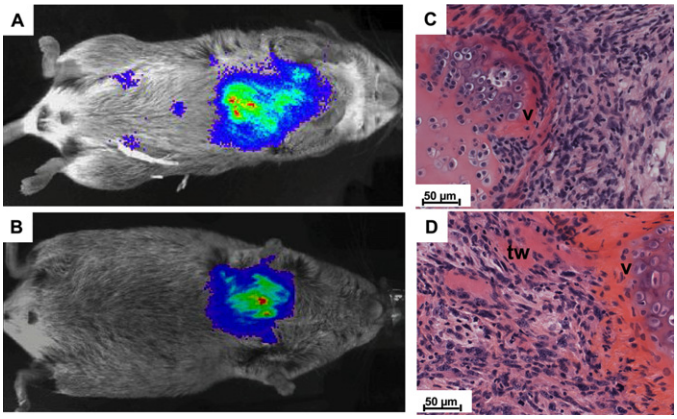

Figure 7. Noninvasive Follow-Up of Spontaneous Murine MM Development

(A) After crossing in a luciferase reporter allele (LucR), we followed MM development in both *Nf2*$^{F/F}$;*p53*$^{F/F}$ and *Nf2*$^{F/F}$;*p53*$^{F/F}$;*Ink4a*$^{*/*}$ mice noninvasively. An example of a bioluminescent primary tumor is shown at 9 weeks after IT injection of Adeno-Cre virus. (B) A LucR^{+} clonal cell line derived from the primary tumor shown in (A) gave LcR^{+} tumors upon orthotopic grafting into syngeneic hosts. Upon histological examination on H&E-stained sections, both primary (C) and orthotopic tumor (D) showed the same invasive growth characteristics (invasive growth into thoracic wall, tw; vertebrae, v). Bars for different magnifications are shown as burn in marks (Axiocam, Color-CCD camera).

expression of Cre recombinase via intrathoracic Adeno-Cre injection in mice. We used homozygously floxed conditional single (*Nf2*, *Ink4a/Arf*, and *p53*) and compound *Nf2*;*Ink4a/Arf*, *Nf2*;*p53*, and *Nf2*;*p53*;*Ink4a*$^{*/*}$ alleles and heterozygously floxed littermates. Although a range of different tumors were found in the conditional mutants due to either infection of tissues other than the mesothelial lining or to other tumor types developing intrathoracically, the vast majority of the mice developed MM. The most common sites for MM development were the visceral pleura of lungs and heart. The sites for secondary or locally metastasized MM development were parietal pleura of diaphragm and thoracic chest wall.

Comparison of MM in Man and Mouse and the Role of Asbestos

Our analysis was driven by the lack of good mouse models that have hampered a thorough understanding of the molecular mechanisms underlying MM. This has allowed us to define the TSG that, upon loss of function, give rise to sporadic MM and to compare the histopathological phenotypes with asbestos-induced MM in mouse and man. Little is known about the (histo)-pathology of murine MM induced by SV40 T antigen or asbestos (Craighead et al., 1987; Topov and Kolev, 1987). Recently, it has been shown that intraperitoneal asbestos exposure of *Nf2*$^{WT/-}$ mice leads to peritoneal MM. These tumors exhibit features of human MM and arise with a median latency of 300 days (Altomare et al., 2005). Since a diversity of tumors has been found in *Nf2*$^{WT/-}$ mice either with or without metastasizing capacities (Giovannini et al., 1999, 2000; McClatchey et al., 1998), it was necessary to clearly distinguish the murine MM from other thoracic sarcomatoid tumors. To make this distinction, we used a panel of histological markers that included panKeratin, N-Cadherin, mesothelin, calretinin, vimentin, MCM-7, SMA, S-100, TTF-1, and Myf-4 supplemented with PTAH and Alcian Blue staining.

The murine MM latency curves indicated that loss of Nf2, p53, and Ink4a/Arf each substantially contribute to MM development. Inclusion of the conventional *Ink4a*$^{*/*}$ (Krimpenfort et al., 2001) knockout allele in the *Nf2*$^{F/F}$;*p53*$^{F/F}$ mice significantly reduced the latency period. MM in both *Nf2*$^{F/F}$;*p53*$^{F/F}$;*Ink4a*$^{*/*}$ as well as in *Nf2*$^{F/F}$;*p53*$^{F/F}$;*Ink4a*$^{*/WT}$ mice presented as multiple tumors of epithelial, mixed, and sarcomatoid phenotype. Moreover, all these fast occurring epitheloid and sarcomatoid MM were highly invasive in both parietal and visceral pleura, this in contrast to the tumors induced in *Nf2*$^{F/F}$;*p53*$^{F/F}$ mice. We conclude that *Ink4a* loss confers a more aggressive invasive phenotype to murine MM.

Whereas in humans a preponderance of the epithelial type of MM opposed to sarcomatoid and mixed type is found, the epitheloid tumors do tend to become invasive in the final stages of the disease. In our mice models, pure epithelial MM were found in *Nf2*$^{F/F}$;*p53*$^{F/F}$ and *Nf2*$^{F/F}$;*Ink4a/Arf*$^{F/F}$ mice, but not in *Nf2*$^{F/F}$;*p53*$^{F/F}$;*Ink4a*$^{*/*}$ mice. Sarcomatoid and mixed MM were found in all three experimental groups. The mixed tumors in *Nf2*$^{F/F}$;*p53*$^{F/F}$;*Ink4a*$^{*/*}$ mice exhibited features of epitheloid MM with large cytoplasmic vacuolization or "signet cell differentiation," which is often observed in epithelial-type MM as well as sarcomatoid MM traversing parietal pleura, i.e., thoracic wall and diaphragm. Likely, the predominant epithelial MM type seen in man opposed to mice may occur as a result of species-specific differences or relate to the route of induction, i.e., the long latency for MM development as a result of asbestos exposure in humans opposed to somatically induced (homozygous) mutations in specific genetic loci in mice.

The Cre-induced biallelic loss of *Nf2* in the mesothelial lining of *Nf2*$^{F/F}$;*p53*$^{F/F}$ and *Nf2*$^{F/F}$;*p53*$^{F/F}$;*Ink4a*$^{*/*}$ CKO mice results in a shorter latency than seen in *Nf2*$^{F/F}$;*Ink4a/Arf*$^{F/F}$ CKO mice, which exhibits a comparable latency as asbestos-induced MM in mice heterozygous for *Nf2*. In two separate studies, intraperitoneal asbestos experiments with mice heterozygous for *Nf2* resulted in MM within 6 months (Fleury-Feith et al., 2003) and 10 months (Altomare et al., 2005) after exposure. In both cases, MM formation was associated with loss of the WT *NF2* allele, and in the latter, most interestingly, tumors had either lost the *Ink4a/Arf* locus or the *p53* locus. These results imply that loss of the WT *Nf2* allele may occur rapidly in conjunction with asbestos exposure and that asbestos may have multiple intracellular genotoxic effects, e.g., loss of *Ink4a/Arf* locus.

How then does asbestos induce MM? Since loss of p16^{INK4A} and NF2 function is frequently observed in human MM, it seems likely that the mechanical and oxidative damage inflicted by asbestos fibers can bring about multiple genetic lesions of which loss of *NF2* and the *INK4A/ARF* locus appear critical. The relevance of NF2 is further supported by the supposedly enhanced susceptibility of an NF2 patient to asbestos-induced mesothelioma (Baser et al., 2002).

Contribution of the Different Genetic Loci to Murine MM Development

Examination of Cre-mediated gene inactivation in tumors showed variable deletion frequencies of *Nf2*, *Ink4a/Arf*, and *p53* alleles. In contrast, complete Cre-mediated gene inactivation was found upon ex vivo propagation of MM, suggesting incomplete deletion found in whole tumor DNA was a result of contamination with WT cells. This stromal compartment was lost during subcloning to derive cell lines. When tumors were induced in mice carrying one WT allele of either *Nf2*, *Ink4a/Arf*, or *p53*, we observed almost invariably loss of the WT allele by LOH. Even in tumors from $Nf2^{F/F}$;$p53^{F/F}$;$Ink4a^{*/WT}$ mice, we observed in a number of instances loss of the *Ink4a* WT allele. Therefore, LOH analyses of tumors that arose in various mutant backgrounds unequivocally demonstrate the importance of loss of *Nf2*, *Ink4a*, and *p53* for MM formation in line with the notion that this model mimics human MM well (Carbone et al., 1997; Lechner et al., 1997; Murthy and Testa, 1999; Papp et al., 2001; Bianchi et al., 1995; Sekido et al., 1995).

Fleury-Feith et al. showed that hemizygosity of *Nf2* was associated with increased susceptibility to asbestos-induced peritoneal tumors, including LOH of *Nf2* in several asbestos-induced neoplastic ascitic fluids (Fleury-Feith et al., 2003). Likewise, Altomare et al., showed in asbestos-exposed *Nf2* (+/−) mice markedly accelerated MM tumor formation compared with asbestos-treated WT littermates. Loss of the WT *Nf2* allele, leading to biallelic inactivation, was observed in all asbestos-induced MM from *Nf2* (+/−) mice and in half of the asbestos-exposed WT mice (Altomare et al., 2005). Our conditional model shows that concomitant loss of *Ink4a/Arf* or *p53* on top of *Nf2* is sufficient to induce MM development without requiring asbestos exposure, suggesting that mutations in *Nf2*, in combination with loss of *Ink4a/Arf* or *p53*, are critical events in MM development, in accordance with the lesions observed in these genes in human MM.

Our observations in mice closely mimic the observations in man in which loss of these same genes is frequently seen (Bianchi et al., 1995; Sekido et al., 1995). Loss of the *NF2* and *INK4A/ARF* loci are often associated with asbestos-induced MM. Comparing the $Nf2^{F/F}$;$Ink4a/Arf^{F/F}$ cohort to the $Nf2^{F/F}$;$p53^{F/F}$;$Ink4a^{*/*}$ cohort allows us to define differences in the consequences of *Arf* and *p53* loss on murine MM development in a *Nf2*;*Ink4a* null background. The reasons to include a *p53* conditional allele were several fold. It allows us to define differences between *p53* and *Arf* loss in a well-defined tumor model. This is an issue of general relevance. Second, from different systems we know that *p53* loss results in an increased genomic instability. In a way, this would make it easier to score for chromosomal changes that otherwise are induced by asbestos. Third, it permits us to evaluate whether *p53* deficiency would make these tumors more refractory to DNA-damaging drugs than tumors with *Arf* inactivation. If this were the case one might exploit this feature therapeutically by exploring DNA damage as part of the intervention strategy in the mostly p53-proficient MM.

Although SV40 T-Ag alone can induce MM in rodents (Adamson et al., 1993; De Luca et al., 1997; Marsella et al., 1997) it remains questionable to what extent this alternative route of MM induction represents a useful model for MM in man. A recent publication did show the synergistic effects of mesothelin-driven SV40-T-Ag expression and asbestos exposure (Robinson et al., 2006). The fact that *Ink4a* loss clearly contributes to MM development, whereas an effect on tumorigenicity was not seen for *Rb* in combination with *Nf2* alone (see Supplemental Data, Table S2), suggests that (also) inactivation of other pocket proteins might be required for MM development, although we did not analyze the effect of *Rb* loss in $Nf2^{F/F}$;$p53^{F/F}$ CKO mice. The strong effect of *Nf2* loss on MM development may relate to the unique nature of the mesothelial cell layer in which control of cell proliferation and differentiation relies on cell surface signaling cues in which *Nf2* plays a critical role. In this respect, it will be of interest to study whether loss or overexpression of other components that interact with *NF2* or act downstream of *Nf2* can modulate MM development. Recent work has shown that reexpression of *Nf2* both inhibits cell proliferation via repression of cyclin D1 (Xiao et al., 2005) and impairs cell spreading and invasiveness by attenuating *FAK* activity (Poulikakos et al., 2006). It will be of interest to determine cyclin D1 levels and the invasive phenotype of our MM cell lines after reexpression of functional *Nf2*.

An Unexpected Role of Ink4a Loss on Murine MM Development

Most of the nodular tumors stained strongly positive for $p16^{Ink4a}$ in the nucleus. In some $Ink4a^{WT/WT}$ and $Ink4a^{*/WT}$ tumors, $p16^{Ink4a}$ expression was lost when the cells invaded the parietal pleura. However, we also observed invading tumors that still exhibited a strong patchy nuclear staining. Therefore, although $p16^{Ink4a}$ loss of function is frequently associated with increased malignancy, the correlation is not seen in all cases, and no consistent change in $p16^{Ink4a}$ expression is observed at the invading front. While loss of $p16^{Ink4a}$ seems to facilitate invasive growth, there are apparent other routes to invasiveness. Our observations in mice carrying either the *Ink4a/Arf* CKO or the *Ink4a** allele support the notion that loss of *Ink4a* is one of the factors that may contribute to the more invasive behavior of murine MM cells. Similar observations were made in the malignant progression caused by *Ink4a/Arf* loss in a model of metastatic pancreatic adenocarcinoma (Aguirre et al., 2003).

In conclusion, we have established a murine model for human MM. Tumors develop after a short latency period in the vast majority of the mice and can be followed noninvasively using bioluminescence imaging. This will serve as a starting point to identify additional recurrent genetic changes and distinct expression characteristics that might define new pathways that are critical for MM development and allow us to design better intervention strategies for this devastating cancer. We have derived a series of cell lines that reproduce the disease upon orthotopic intrathoracic grafting. These may facilitate these studies.

EXPERIMENTAL PROCEDURES

Nf2, *p53*, and *Ink4a/Arf* Conditional and *Ink4a* Functional Knockout Mice

Nf2, *p53*, and *Ink4a/Arf* conditional and *Ink4a* functional knockout mice (*Ink4a**) have been described earlier (Giovannini et al., 2000; Marino et al., 2000; Krimpenfort et al., 2001). All animal experiments performed in this manuscript have been approved by our local animal experimental committee (DEC NKI). (For details on genotyping see the Supplemental Experimental Procedures.)

Generation and Purification of Adeno-Cre Virus

The Adeno-Cre virus was constructed and propagated as described (Anton and Graham, 1995). (For details see Supplemental Experimental Procedures.)

Recombination of the Mesothelial Cell Linings In Vivo

Rosa26R reporter mice (Soriano, 1999) or WT FVB/N mice were injected intrathoracically with 1×10^9 pfu of Adeno-Cre or Adeno-LacZ virus to test for the efficiency of infection and Cre-mediated recombination of R26R in mesothelial cells in vivo. After 7 days, mice were sacrificed and organs were processed for β-galactosidase staining (Akagi et al., 1997). Tissues were paraffin embedded, sectioned, and counterstained with neutral red.

Intrathoracic Injections of Adeno-Cre Virus

Nf2, *p53*, *Ink4a/Arf* conditional, and *Ink4a** knockout mice were crossed to generate different sets of compound CKO mice. As a control, we used FVB/N mice. The experimental groups were injected IT with 2 to 5 × 10^8 Adeno-Cre virus particles. In short, we filled insulin injection needles with 50 μl virus suspension (2–5 × 10^8 pfu/50 μl) and put them on a heat sheet. We then anesthesized the mice with either isoflurane, or if no isoflurane anesthesia equipment was available, mice were temporarily sedated by i.p. injections with Ketamine:Sedacine:NaCl (2:1:17) mixture, 100 μl per 10 g mouse. When sedated, mice were fixed on their back with thumb and pointing finger behind head (pointing toward left side), so that the chest is in a fixed position. Injection site was cleaned with alcohol (70%), and carefully, 50 μl of virus suspension was injected in between ribs inside the chest (needle penetrates chest wall from 2 to 3 mm). There was a low morbidity associated with IT injection (<2%).

IHC Analysis of the Tumors

The injected mice were monitored biweekly for the development of tumors and general health status. Mice were sacrificed when signs of discomfort became evident. Tissues from the site of Adeno-Cre injection were collected for pathological examination, and part of the tumors was stored at −80°C. The formalin fixed material was sectioned, H&E stained, and analyzed microscopically. (For a detailed description, see Supplemental Experimental Procedures.)

Southern Blot Analysis for Cre-Mediated Loss or Loss of Heterozygosity for *Nf2*, *p53*, and *Ink4a/Arf*

Tumor DNA was isolated by proteinase K treatment in lysis buffer and extracted once with buffered phenol:chloroform:isoamylalcohol (24:24:2) and once with chloroform and precipitated with ethanol:water (2:1) (Laird et al., 1991). *Nf2* LOH analysis was performed by Southern blotting of BamHI/XbaI digested DNA and hybridization to the 221 bp PCR probe-B (Giovannini et al., 2000). For *p53*, we used BglII-digested DNA hybridized to the *Trp53* 5′ XbaI probe which is a 700 nt genomic XbaI fragment subcloned in pBSK and labeled by PCR (Jonkers et al., 2001; Vooijs et al., 2001). For the *Ink4a* probe, we cut probe B that is identical to the 1.3 kb BamHI probe described by Serrano et al. in two parts by using the restriction enzyme XbaI (Serrano et al., 1996). From the two resulting fragments, we hybridyzed the 500 bp fragment on Southern blots of PsiI digested DNA.

$p16^{Ink4a}$ Expression Study

$p16^{Ink4a}$ expression was studied in representative tumors from all experimental groups to analyze a possible correlation of *Ink4a* loss with invasive tumor growth behavior. Therefore, we stained several tumor sections with an $p16^{Ink4a}$ antibody (Sc1207, clone M-156, Santa Cruz) as performed for other antibodies in the section above. $p16^{Ink4a}$ staining was scored as either positive nuclear staining or cytoplasmic staining or completely negative.

In Vivo Imaging of Murine MM Development in $Nf2^{F/F}$;$p53^{F/F}$(;$Ink4a^{*/*}$) Mice

$Nf2^{F/F}$;$p53^{F/F}$(;$Ink4a^{*/*}$) mice were intercrossed with LucR mice to generate LucR;$Nf2^{F/F}$;$p53^{F/F}$(;$Ink4a^{*/*}$) mice. After IT injection of Adeno-Cre, the mice were imaged at fixed 1 week time intervals on the Xenogen IVIS 100 Imaging System (Xenogen Corporation, Alameda, California) optimized for in vivo (whole, living animals) imaging. Photon emission was used as a measure of tumor load. Mice were sacrificed according to the same criteria used for $Nf2^{F/F}$;$p53^{F/F}$(;$Ink4a^{*/*}$) mice.

SUPPLEMENTAL DATA

The Supplemental Data include two supplemental tables and Supplemental Experimental Procedures and can be found with this article online at http://www.cancercell.org/cgi/content/full/13/3/261/DC1/.

ACKNOWLEDGMENTS

We thank Jos Jonkers, Sabine Linn, and Paul Baas for their contributions to this project and discussions. The pKER antibody was a gift from Gert Schaart and Frans Raemakers (Department of Molecular Biology, University of Maastricht.). We thank Frank Matthesius for assisting in the genotyping of the mice. We are indebted to our colleagues of the NKI animal facility for animal husbandry and especially Loes van Rijswijk, and Fina van der Ahe for the Adeno-Cre virus injections and the Animal pathology department.

We hereby state that we do not have any conflict of interests. J.J., E.v.M, and M.V. have been supported by a grant from the Dutch Cancer Society (*NKI 99-2058*).

Received: September 6, 2007
Revised: December 24, 2007
Accepted: January 25, 2008
Published: March 10, 2008

REFERENCES

Adamson, I., Bakowska, J., and Bowden, D. (1993). Mesothelial cell proliferation after instillation of long or short asbestos fibers into mouse lung. Am. J. Pathol. *142*, 1209–1216.

Aguirre, A.J., Bardeesy, N., Sinha, M., Lopez, L., Tuveson, D.A., Horner, J., Redston, M.S., and DePinho, R.A. (2003). Activated Kras and Ink4a/Arf deficiency cooperate to produce metastatic pancreatic ductal adenocarcinoma. Genes Dev. *17*, 3112–3126.

Akagi, K., Sandig, V., Vooijs, M., Van der Valk, M., Giovannini, M., Strauss, M., and Berns, A. (1997). Cre-mediated somatic site-specific recombination in mice. Nucleic Acids Res. *25*, 1766–1773.

Altomare, D.A., Vaslet, C.A., Skele, K.L., De Rienzo, A., Devarajan, K., Jhanwar, S.C., McClatchey, A.I., Kane, A.B., and Testa, J.R. (2005). A mouse model recapitulating molecular features of human mesothelioma. Cancer Res. *65*, 8090–8095.

Anton, M., and Graham, F. (1995). Site-specific recombination mediated by an adenovirus vector expressing the Cre recombinase protein: A molecular switch for control of gene expression. J. Virol. *69*, 4600–4606.

Ascoli, V., Aalto, Y., Carnovale-Scalzo, C., Nardi, F., Falzetti, D., Mecucci, C., and Knuutila, S. (2001). DNA copy number changes in familial malignant mesothelioma. Cancer Genet. Cytogenet. *127*, 80–82.

Attanoos, R.L., Dojcinov, S.D., Webb, R., and Gibbs, A.R. (2000). Antimesothelial markers in sarcomatoid mesothelioma and other spindle cell neoplasms. Histopathology *37*, 224–231.

Baser, M.E., De Rienzo, A., Altomare, D., Balsara, B.R., Hedrick, N.M., Gutmann, D.H., Pitts, L.H., Jackler, R.K., and Testa, J.R. (2002). Neurofibromatosis 2 and malignant mesothelioma. Neurology *59*, 290–291.

Bianchi, A., Mitsunaga, S., Cheng, J., Klein, W., Jhanwar, S., Seizinger, B., Kley, N., Klein-Szanto, A., and Testa, J. (1995). High frequency of inactivating mutations in the neurofibromatosis type 2 gene (NF2) in primary malignant mesotheliomas. Proc. Natl. Acad. Sci. USA *92*, 10854–10858.

Bianchi, A.B., Hara, T., Ramesh, V., Gao, J., Klein-Szanto, A.J., Morin, F., Menon, A.G., Trofatter, J.A., Gusella, J.F., Seizinger, B.R., et al. (1994). Mutations in transcript isoforms of the neurofibromatosis 2 gene in multiple human tumour types. Nat. Genet. *6*, 185–192.

Brault, E., Gautreau, A., Lamarine, M., Callebaut, I., Thomas, G., and Goutebroze, L. (2001). Normal membrane localization and actin association of the NF2 tumor suppressor protein are dependent on folding of its N-terminal domain. J. Cell Sci. *114*, 1901–1912.

Cagle, P.T., Truong, L.D., Roggli, V.L., and Greenberg, S.D. (1989). Immunohistochemical differentiation of sarcomatoid mesotheliomas from other spindle cell neoplasms. Am. J. Clin. Pathol. *92*, 566–571.

Carbone, M., Rizzo, P., Grimley, P.M., Procopio, A., Mew, D.J., Shridhar, V., de Bartolomeis, A., Esposito, V., Giuliano, M.T., Steinberg, S.M., et al. (1997). Simian virus-40 large-T antigen binds p53 in human mesotheliomas. Nat. Med. *3*, 908–912.

Carter, D., and Otis, C.N. (1988). Three types of spindle cell tumors of the pleura. Fibroma, sarcoma, and sarcomatoid mesothelioma. Am. J. Surg. Pathol. *12*, 747–753.

Cheng, J.Q., Jhanwar, S.C., Klein, W.M., Bell, D.W., Lee, W.C., Altomare, D.A., Nobori, T., Olopade, O.I., Buckler, A.J., and Testa, J.R. (1994). p16 alterations and deletion mapping of 9p21-p22 in malignant mesothelioma. Cancer Res. *54*, 5547–5551.

Cicala, C., Pompetti, F., and Carbone, M. (1993). SV40 induces mesotheliomas in hamsters. Am. J. Pathol. *142*, 1524–1533.

Claudio, J., Lutchman, M., and Rouleau, G. (1995). Widespread but cell type-specific expression of the mouse neurofibromatosis type 2 gene. Neuroreport *6*, 1942–1946.

Claudio, J.O., Malo, D., and Rouleau, G.A. (1994a). The mouse neurofibromatosis type 2 gene maps to chromosome 11. Genomics *21*, 437–439.

Claudio, J.O., Marineau, C., and Rouleau, G.A. (1994b). The mouse homologue of the neurofibromatosis type 2 gene is highly conserved. Hum. Mol. Genet. *3*, 185–190.

Craighead, J.E., Akley, N.J., Gould, L.B., and Libbus, B.L. (1987). Characteristics of tumors and tumor cells cultured from experimental asbestos-induced mesotheliomas in rats. Am. J. Pathol. *129*, 448–462.

De Luca, A., Baldi, A., Esposito, V., Howard, C.M., Bagella, L., Rizzo, P., Caputi, M., Pass, H.I., Giordano, G.G., Baldi, F., et al. (1997). The retinoblastoma gene family pRb/p105, p107, pRb2/p130 and simian virus-40 large T-antigen in human mesotheliomas. Nat. Med. *3*, 913–916.

De Rienzo, A., Balsara, B.R., Apostolou, S., Jhanwar, S.C., and Testa, J.R. (2001). Loss of heterozygosity analysis defines a 3-cM region of 15q commonly deleted in human malignant mesothelioma. Oncogene *20*, 6245–6249.

Deguen, B., Merel, P., Goutebroze, L., Giovannini, M., Reggio, H., Arpin, M., and Thomas, G. (1998). Impaired interaction of naturally occurring mutant NF2 protein with actin-based cytoskeleton and membrane. Hum. Mol. Genet. *7*, 217–226.

den Bakker, M.A., Riegman, P.H., Suurmeijer, A.P., Vissers, C.J., Sainio, M., Carpen, O., and Zwarthoff, E.C. (2000). Evidence for a cytoskeleton attachment domain at the N-terminus of the NF2 protein. J. Neurosci. Res. *62*, 764–771.

Fleury-Feith, J., Lecomte, C., Renier, A., Matrat, M., Kheuang, L., Abramowski, V., Levy, F., Janin, A., Giovannini, M., and Jaurand, M.C. (2003). Hemizygosity of Nf2 is associated with increased susceptibility to asbestos-induced peritoneal tumours. Oncogene *22*, 3799–3805.

Giovannini, M., Robanus-Maandag, E., Niwa-Kawakita, M., van der Valk, M., Woodruff, J.M., Goutebroze, L., Merel, P., Berns, A., and Thomas, G. (1999). Schwann cell hyperplasia and tumors in transgenic mice expressing a naturally occurring mutant NF2 protein. Genes Dev. *13*, 978–986.

Giovannini, M., Robanus-Maandag, E., van der Valk, M., Niwa-Kawakita, M., Abramowski, V., Goutebroze, L., Woodruff, J.M., Berns, A., and Thomas, G. (2000). Conditional biallelic Nf2 mutation in the mouse promotes manifestations of human neurofibromatosis type 2. Genes Dev. *14*, 1617–1630.

Gusella, J.F., Ramesh, V., MacCollin, M., and Jacoby, L.B. (1999). Merlin: The neurofibromatosis 2 tumor suppressor. Biochim. Biophys. Acta *1423*, M29–M36.

Gutmann, D.H., Geist, R.T., Xu, H., Kim, J.S., and Saporito-Irwin, S. (1998). Defects in neurofibromatosis 2 protein function can arise at multiple levels. Hum. Mol. Genet. *7*, 335–345.

Gutmann, D.H., Sherman, L., Seftor, L., Haipek, C., Hoang Lu, K., and Hendrix, M. (1999). Increased expression of the NF2 tumor suppressor gene product, merlin, impairs cell motility, adhesionand spreading. Hum. Mol. Genet. *8*, 267–275.

Hodgson, J.T., McElvenny, D.M., Darnton, A.J., Price, M.J., and Peto, J. (2005). The expected burden of mesothelioma mortality in Great Britain from 2002 to 2050. Br. J. Cancer *92*, 587–593.

Hubner, R., and Van Marck, E. (2002). Reappraisal of the strong association between simian virus 40 and human malignant mesothelioma of the pleura (Belgium). Cancer Causes Control *13*, 121–129.

Jackson, E.L., Willis, N., Mercer, K., Bronson, R.T., Crowley, D., Montoya, R., Jacks, T., and Tuveson, D.A. (2001). Analysis of lung tumor initiation and progression using conditional expression of oncogenic K-ras. Genes Dev. *15*, 3243–3248.

Jonkers, J., and Berns, A. (2002). Conditional mouse models of sporadic cancer. Nat. Rev. Cancer *2*, 251–265.

Jonkers, J., Meuwissen, R., van der Gulden, H., Peterse, H., van der Valk, M., and Berns, A. (2001). Synergistic tumor suppressor activity of BRCA2 and p53 in a conditional mouse model for breast cancer. Nat. Genet. *29*, 418–425.

Khalidi, H.S., Medeiros, L.J., and Battifora, H. (2000). Lymphohistiocytoid mesothelioma. An often misdiagnosed variant of sarcomatoid malignant mesothelioma. Am. J. Clin. Pathol. *113*, 649–654.

Kissil, J.L., Johnson, K.C., Eckman, M.S., and Jacks, T. (2002). Merlin phosphorylation by p21-activated kinase 2 and effects of phosphorylation on merlin localization. J. Biol. Chem. *277*, 10394–10399.

Knudson, A. (1995). Asbestos and mesothelioma: Genetic lessons from a tragedy. Proc. Natl. Acad. Sci. USA *92*, 10819–10820.

Krimpenfort, P., Quon, K.C., Mooi, W.J., Loonstra, A., and Berns, A. (2001). Loss of p16Ink4a confers susceptibility to metastatic melanoma in mice. Nature *413*, 83–86.

Laird, P.W., Zijderveld, A., Linders, K., Rudnicki, M.A., Jaenisch, R., and Berns, A. (1991). Simplified mammalian DNA isolation procedure. Nucleic Acids Res. *19*, 4293.

Lechner, J.F., Tesfaigzi, J., and Gerwin, B.I. (1997). Oncogenes and tumor-suppressor genes in mesothelioma–a synopsis. Environ. Health Perspect. *105*, 1061–1067.

Lee, W.C., and Testa, J.R. (1999). Somatic genetic alterations in human malignant mesothelioma. Int. J. Oncol. *14*, 181–188.

Libbus, B.L., Craighead, J.E., Akley, N.J., and Gould, L.B. (1988). Chromosomal translocations with specific breakpoints in asbestos-induced rat mesotheliomas. Cancer Res. *48*, 6455–6461.

Liu, W., Ernst, J.D., and Courtney Broaddus, V. (2000). Phagocytosis of crocidolite asbestos induces oxidative stress, DNA damage, and apoptosis in mesothelial cells. Am. J. Respir. Cell Mol. Biol. *23*, 371–378.

Loonstra, A., Vooijs, M., Beverloo, H., Allak, B., van Drunen, E., Kanaar, R., Berns, A., and Jonkers, J. (2001). Growth inhibition and DNA damage induced by Cre recombinase in mammalian cells. Proc. Natl. Acad. Sci. USA *98*, 9209–9214.

Lopos-Rios, F., Illei, P.B., Rusch, V., and Ladanyi, M. (2004). Evidence against the role for SV40 infection in human mesothelioma and high risk of false positive PCR results owing to the presence of SV40 sequences in common laboratory plasmids. Lancet *364*, 1159–1166.

Lyons, S.K., Meuwissen, R., Krimpenfort, P., and Berns, A. (2003). The generation of a conditional reporter that enables bioluminescence imaging of Cre/loxP-dependent tumorigenesis in mice. Cancer Res. *63*, 7042–7046.

Marino, S., Vooijs, M., van der Gulden, H., Jonkers, J., and Berns, A. (2000). Induction of medulloblastomas in p53-null mutant mice by somatic inactivation of Rb in the external granular layer cells of the cerebellum. Genes Dev. *14*, 994–1004.

Marsella, J.M., Liu, B.L., Vaslet, C.A., and Kane, A.B. (1997). Susceptibility of p53-deficient mice to induction of mesothelioma by crocidolite asbestos fibers. Environ. Health Perspect. *105*, 1069–1072.

McClatchey, A.I., Saotome, I., Mercer, K., Crowley, D., Gusella, J.F., Bronson, R.T., and Jacks, T. (1998). Mice heterozygous for a mutation at the Nf2 tumor suppressor locus develop a range of highly metastatic tumors. Genes Dev. *12*, 1121–1133.

McClatchey, A.I., Saotome, I., Ramesh, V., Gusella, J.F., and Jacks, T. (1997). The Nf2 tumor suppressor gene product is essential for extraembryonic development immediately prior to gastrulation. Genes Dev. *11*, 1253–1265.

Meuwissen, R., Jonkers, J., and Berns, A. (2001). Mouse Models for Sporadic Cancer. Exp. Cell Res. *264*, 100–110.

Mor, O., Yaron, P., Huszar, M., Yellin, A., Jakobovitz, O., Brok-Simoni, F., Rechavi, G., and Reichert, N. (1997). Absence of p53 mutations in malignant mesotheliomas. Am. J. Respir. Cell Mol. Biol. *16*, 9–13.

Morrison, H., Sherman, L.S., Legg, J., Banine, F., Isacke, C., Haipek, C.A., Gutmann, D.H., Ponta, H., and Herrlich, P. (2001). The NF2 tumor suppressor gene product, merlin, mediates contact inhibition of growth through interactions with CD44. Genes Dev. *15*, 968–980.

Morrison, H., Sperka, T., Manent, J., Giovannini, M., Ponta, H., and Herrlich, P. (2007). Merlin/neurofibromatosis type 2 suppresses growth by inhibiting the activation of Ras and Rac. Cancer Res. *67*, 520–527.

Murthy, S.S., and Testa, J.R. (1999). Asbestos, chromosomal deletions, and tumor suppressor gene alterations in human malignant mesothelioma. J. Cell. Physiol. *180*, 150–157.

Ordonez, N.G. (1999). Role of immunohistochemistry in differentiating epithelial mesothelioma from adenocarcinoma. Review and update. Am. J. Clin. Pathol. *112*, 75–89.

Ordonez, N.G., and Tornos, C. (1997). Malignant peripheral nerve sheath tumor of the pleura with epithelial and rhabdomyoblastic differentiation: Report of a case clinically simulating mesothelioma. Am. J. Surg. Pathol. *21*, 1515–1521.

Papp, T., Schipper, H., Pemsel, H., Bastrop, R., Muller, K.M., Wiethege, T., Weiss, D.G., Dopp, E., Schiffmann, D., and Rahman, Q. (2001). Mutational analysis of N-ras, p53, p16INK4a, p14ARF and CDK4 genes in primary human malignant mesotheliomas. Int. J. Oncol. *18*, 425–433.

Poulikakos, P.I., Xiao, G.H., Gallagher, R., Jablonski, S., Jhanwar, S.C., and Testa, J.R. (2006). Re-expression of the tumor suppressor NF2/merlin inhibits invasiveness in mesothelioma cells and negatively regulates FAK. Oncogene *25*, 5960–5968.

Prins, J.B., Williamson, K.A., Kamp, M.M., Van Hezik, E.J., Van der Kwast, T.H., Hagemeijer, A., and Versnel, M.A. (1998). The gene for the cyclin-dependent-kinase-4 inhibitor, CDKN2A, is preferentially deleted in malignant mesothelioma. Int. J. Cancer *75*, 649–653.

Rizzo, P., Bocchetta, M., Powers, A., Foddis, R., Stekala, E., Pass, H.I., and Carbone, M. (2001). SV40 and the pathogenesis of mesothelioma. Semin. Cancer Biol. *11*, 63–71.

Robinson, C., van Bruggen, I., Segal, A., Dunham, M., Sherwood, A., Koentgen, F., Robinson, B.W., and Lake, R.A. (2006). A novel SV40 TAg transgenic model of asbestos-induced mesothelioma: Malignant transformation is dose dependent. Cancer Res. *66*, 10786–10794.

Rouleau, G., Merel, P., Lutchman, M., Sanson, M., Zucman, J., Marineau, C., Hoang-Xuan, K., Demczuk, S., Desmaze, C., Plougastel, B., et al. (1993). Alteration in a new gene encoding a putative membrane-organizing protein causes neuro-fibromatosis type 2. Nature *363*, 515–521.

Sainio, M., Zhao, F., Heiska, L., Turunen, O., den Bakker, M., Zwarthoff, E., Lutchman, M., Rouleau, G.A., Jaaskelainen, J., Vaheri, A., and Carpen, O. (1997). Neurofibromatosis 2 tumor suppressor protein colocalizes with ezrin and CD44 and associates with actin-containing cytoskeleton. J. Cell Sci. *110*, 2249–2260.

Sandberg, A.A., and Bridge, J.A. (2001). Updates on the cytogenetics and molecular genetics of bone and soft tissue tumors. Cancer Genet Cytogenet *127*, 93–110.

Sandhu, H., Dehnen, W., Roller, M., Abel, J., and Unfried, K. (2000). mRNA expression patterns in different stages of asbestos-induced carcinogenesis in rats. Carcinogenesis *21*, 1023–1029.

Sekido, Y., Pass, H., Bader, S., Mew, D., Christman, M., Gazdar, A., and Minna, J. (1995). Neurofibromatosis type 2 (NF2) gene is somatically mutated in mesothelioma but not in lung cancer. Cancer Res. *55*, 1227–1231.

Serrano, M., Lee, H., Chin, L., Cordon-Cardo, C., Beach, D., and DePinho, R.A. (1996). Role of the INK4a locus in tumor suppression and cell mortality. Cell *85*, 27–37.

Sharpless, E., and Chin, L. (2003). The INK4a/ARF locus and melanoma. Oncogene *22*, 3092–3098.

Sharpless, N.E., Alson, S., Chan, S., Silver, D.P., Castrillon, D.H., and DePinho, R.A. (2002). p16(INK4a) and p53 deficiency cooperate in tumorigenesis. Cancer Res. *62*, 2761–2765.

Shaw, R.J., McClatchey, A.I., and Jacks, T. (1998a). Localization and functional domains of the neurofibromatosis type II tumor suppressor, merlin. Cell Growth Differ. *9*, 287–296.

Shaw, R.J., McClatchey, A.I., and Jacks, T. (1998b). Regulation of the neurofibromatosis type 2 tumor suppressor protein, merlin, by adhesion and growth arrest stimuli. J. Biol. Chem. *273*, 7757–7764.

Sherman, L.S., and Gutmann, D.H. (2001). Merlin: Hanging tumor suppression on the Rac. Trends Cell Biol. *11*, 442–444.

Shibata, H., Toyama, K., Shioya, H., Ito, M., Hirota, M., Hasegawa, S., Matsumoto, H., Takano, H., Akiyama, T., Toyoshima, K., et al. (1997). Rapid colorectal adenoma formation initiated by conditional targeting of the Apc gene. Science *278*, 120–123.

Soriano, P. (1999). Generalized lacZ expression with the ROSA26 Cre reporter strain. Nat. Genet. *21*, 70–71.

Takeshima, H., Izawa, I., Lee, P., Safdar, N., Levin, V., and Saya, H. (1994). Detection of cellular proteins that interact with the NF2 tumor suppressor gene product. Oncogene *9*, 2135–2144.

Tiainen, M., Tammilehto, L., Rautonen, J., Tuomi, T., Mattson, K., and Knuutila, S. (1989). Chromosomal abnormalities and their correlations with asbestos exposure and survival in patients with mesothelioma. Br. J. Cancer *60*, 618–626.

Tikoo, A., Varga, M., Ramesh, V., Gusella, J., and Maruta, H. (1994). An anti-ras function of neurofibromatosis type 2 gene product (NF2/Merlin). J. Biol. Chem. *269*, 23387–23390.

Topov, J., and Kolev, K. (1987). Cytology of experimental mesotheliomas induced with crocidolite asbestos. Acta Cytol. *31*, 369–373.

Trofatter, J.A., MacCollin, M.M., Rutter, J.L., Murrell, J.R., Duyao, M.P., Parry, D.M., Eldridge, R., Kley, N., Menon, A.G., Pulaski, K., et al. (1993). A novel moesin-, ezrin-, radixin-like gene is a candidate for the neurofibromatosis 2 tumor suppressor. Cell *75*, 826.

Vooijs, M., Jonkers, J., and Berns, A. (2001). A highly efficient ligand-regulated Cre recombinase mouse line shows that LoxP recombination is position dependent. EMBO Rep. *2*, 292–297.

Xiao, G.H., Beeser, A., Chernoff, J., and Testa, J.R. (2002). p21-activated kinase links Rac/Cdc42 signaling to merlin. J. Biol. Chem. *277*, 883–886. Published online November 21, 2001. 10.1074/jbc.C100553200.

Xiao, G.H., Gallagher, R., Shetler, J., Skele, K., Altomare, D.A., Pestell, R.G., Jhanwar, S., and Testa, J.R. (2005). The NF2 tumor suppressor gene product, merlin, inhibits cell proliferation and cell cycle progression by repressing cyclin D1 expression. Mol. Cell. Biol. *25*, 2384–2394.